Non-Gaussianity of quantum states: An experimental test on single-photon-added coherent states

Marco Barbieri,[1] Nicolò Spagnolo,[1,2] Marco G. Genoni,[3] Franck Ferreyrol,[1] Rémi Blandino,[1] Matteo G. A. Paris,[3] Philippe Grangier,[1] and Rosa Tualle-Brouri[1]

[1]*Laboratoire Charles Fabry, Institut d'Optique, Université Paris-Sud and CNRS, F-91127, Palaiseau, France*

[2]*Dipartimento di Fisica, "Sapienza" Università di Roma and CNISM, I-00185, Roma, Italy*

[3]*Dipartimento di Fisica dell'Università degli Studi di Milano and CNISM, UdR Milano Università, I-20133 Milano, Italy*

(Received 18 October 2010; published 28 December 2010)

Non-Gaussian states and processes are useful resources in quantum information with continuous variables. An experimentally accessible criterion has been proposed to measure the degree of non-Gaussianity of quantum states based on the conditional entropy of the state with a Gaussian reference. Here we adopt such a criterion to characterize an important class of nonclassical states: single-photon-added coherent states. Our studies demonstrate the reliability and sensitivity of this measure and use it to quantify how detrimental is the role of experimental imperfections in our implementation.

DOI: 10.1103/PhysRevA.82.063833 PACS number(s): 42.50.Ct, 42.50.Dv, 03.65.Wj, 03.67.−a

I. INTRODUCTION AND DEFINITIONS

Quantum information offers a different viewpoint on fundamental aspects of quantum mechanics: it aims to assess and exploit the quantum properties of a physical system as a resource for a different, and hopefully more efficient, treatment of information. Indeed, within the framework of quantum information with continuous variables [1], nonclassical states of the radiation field represent a resource, and much attention has been devoted to their generation schemes, which usually involve nonlinear interaction in optically active media.

On the other hand, the reduction postulate provides an alternative mechanism to achieve effective nonlinear dynamics; if a measurement is performed on a portion of a composite entangled system, the other component is conditionally reduced according to the outcome of the measurement. The resulting dynamics may be highly nonlinear, and may produce quantum states that cannot be generated by currently achievable nonlinear processes. Conditional measurements have been exploited to engineer nonclassical states and, in particular, have been recently employed to obtain non-Gaussian states.

While Gaussian states, defined as states with a Gaussian Wigner function, are known to provide useful resources for tasks such as teleportation [2,3], cloning [4–6], or dense coding [7–9], there is an ongoing effort to study which protocols are allowed by non-Gaussian resources. The most notable example is certainly their use for an optical quantum computer [10,11], alongside their employment for improving teleportation [12–14], cloning [15], and storage [16]. Several implementations of non-Gaussian states have been reported so far, in particular from squeezed light [17–25], close-to-threshold parametric oscillators [26,27] in optical cavities [28], and in superconducting circuits [29]. Non-Gaussian operations are also interesting for tasks such as entanglement distillation [30,31] and noiseless amplification [32,33], which are also obtained in a conditional fashion, accepting only those events heralded by a measurement result.

In principle, non-Gaussianity is not directly related to the nonclassical character of a quantum state and, in turn, a classical non-Gaussian state may be prepared (e.g., by phase-diffusion of coherent states or photon subtraction on thermal states [34]). On the other hand, in the applications mentioned above it is the presence of both non-Gaussianity and nonclassicality which allows for enhancement of performances. Therefore, de-Gaussification protocols of interest for quantum information are those providing non-Gaussianity in conjunction with nonclassicality.

In this work we address the conditional dynamics induced by the so-called photon addition as a protocol to generate nonclassical non-Gaussian states. We quantify experimentally the amount of non-Gaussianity obtained by adding a photon to a coherent state [19,35–37]. Differently from previous investigations [35,38–41], we can explicitly address the two aspects of non-Gaussianity and nonclassicality at once. For the former, we adopt the non-Gaussianity measure $\delta[\varrho]$ proposed in [42,43], which is defined as the quantum relative entropy between the quantum state ϱ itself and a reference Gaussian state τ having the same covariance matrix as ϱ. Given this choice of reference Gaussian state, we have $\mathrm{Tr}[\varrho \ln \tau] = \mathrm{Tr}[\tau \ln \tau]$, as $\ln \tau$ is a polynomial of order at most two in the canonical variables [42,44]. We thus find

$$\begin{aligned}\delta[\varrho] &= \mathcal{S}(\varrho\|\tau) = \mathrm{Tr}\,[\varrho(\ln\varrho - \ln\tau)]\\ &= \mathcal{S}(\tau) - \mathcal{S}(\varrho);\end{aligned} \tag{1}$$

that is, $\delta[\varrho]$ is simply equal to the difference between the von Neumann entropy of τ and the von Neumann entropy of ϱ. In Ref. [42] it has been shown that this measure is nonzero only for non-Gaussian states. It is also additive under tensor product, invariant under unitary Gaussian operations, and in general it does not increase under generic completely positive Gaussian channels. This measure is somehow preferable to that based on the Hilbert-Schmidt distance [45] in a quantum information context, since it is based on an information-related quantity. We note, however, that a mixture (e.g., doubly peaked) of classical states can also be strongly non-Gaussian. We therefore adopt an additional "nonclassicality" criterion.

Several measures of nonclassicality have been proposed in literature [46–49]; for our purposes we consider as a witness a quantity $\nu[\varrho]$ related to the negativity of the Wigner function. This is normalized to a reference, which we choose to be

 ©2010 The American Physical Society

a single-photon state $W_1(x,p)$. The nonclassicality is then defined as

$$\nu[\varrho] = \frac{\min[W(x,p)]}{\min[W_1(x,p)]}. \tag{2}$$

This reference has been chosen since it has the lowest value within the class of states we consider. While this does not constitute a measure, it acts as a witness for nonclassical states whenever $\nu[\varrho] > 0$. The choice of using the single photon as a reference is dictated by the need of a measure which does not depend on the convention for the quadratures. Moreover, it sets to unity the highest value of $\nu[\varrho]$ attainable in the class of states under investigation.

II. EXPERIMENT

A conceptual scheme of the experiment is shown in Fig. 1. A coherent input beam $|\alpha\rangle$ is injected in an optical parametric amplifier (OPA). This is a three-wave nonlinear interaction between a pump beam and the input beam (usually called the signal s) which results in the generation of a third beam called the idler (i). When the pump is an intense beam, we can treat it as a classical field: the output state of the s and i modes can then be expressed as the application of the squeezing operator

$$S_{s,i}(r) = \exp[r(a_s^\dagger a_i^\dagger - a_i a_s)] \tag{3}$$

to the input $|\alpha\rangle_s|0\rangle_i$. Here, r is the squeezing parameter, which depends on the pump intensity, the crystal length, and its nonlinear coefficients, and which attained a value $r \simeq 0.105$ in our experiment. We can then approximate $S_{s,i}(r)$ by taking the limit of weak nonlinearity:

$$S_{s,i}(r) \simeq I + r(a_s^\dagger a_i^\dagger) - r(a_i a_s). \tag{4}$$

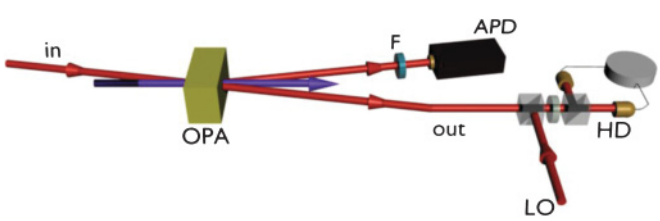

FIG. 1. (Color online) Layout of the experiment. An optical parametric amplifier (OPA) is injected with a coherent state of variable amplitude $\|\alpha\|$ in the range [0,1.5]. This is realized by a 100-μm-thick slab of potassium niobate, pumped by a frequency-doubled mode-locked Ti:sapphire laser ($\lambda_p = 425$ nm, pulse duration 230 fs, repetition rate 800 kHz). Our OPA is driven in the frequency-degenerate and noncollinear regime to generate an idler at the same wavelength $\lambda = 2\lambda_p$ as the coherent seed; this is then spatially filtered with a single-mode fiber, spectrally filtered by a diffraction grating and a slit, indicated as F in the figure. Finally, the idler is detected by an avalanche photodiode APD. The observation of the output conditioned by an APD count results in single-photon addition. The quantum state of the output is reconstructed by homodyne detection (HD). Mode matching with the local oscillator (LO) employs polarization: the signal and the LO are first matched on a polarization beam splitter, and then combined using a half waveplate and a second polariser so to realize an accurate 50 : 50 intensity splitting.

We now put an avalanche photodiode (APD) on the idler beam, and accept only those events when a click is registered. Since the idler was originally in the vacuum state, the only term which can give a contribution to $S_{s,i}(r)$ is the second one. Therefore, the detection of a single photon to the idler heralds the addition of a single photon to the coherent state, transforming it into

$$\frac{1}{\sqrt{1+\|\alpha\|^2}} a^\dagger|\alpha\rangle, \tag{5}$$

in the ideal case. In practice, we need a careful analysis of those processes which spoil the photon addition and the non-Gaussianity of the resulting state. Here, we follow closely the model presented in Refs. [20,23,30].

The detection on the idler beam is performed by an APD that cannot resolve photon number. In the limit of small detection efficiency, we can approximate the detection process as the application of the a_i annihilation operator to the idler mode. This is actually the case in our experiment, where the overall detection efficiency is less than 10% due to spatial filtering ($\lesssim$75%), spectral filtering ($\lesssim$30%), and the limited efficiency of the photodiode (55%).

III. RESULTS AND DISCUSSIONS

In Fig. 2 we plot $\delta[\varrho]$ and $\nu[\varrho]$ as a function of the coherent amplitude α for different values of r. We observe that the two trends resemble each other closely, suggesting that the non-Gaussianity induced by photon addition is essentially

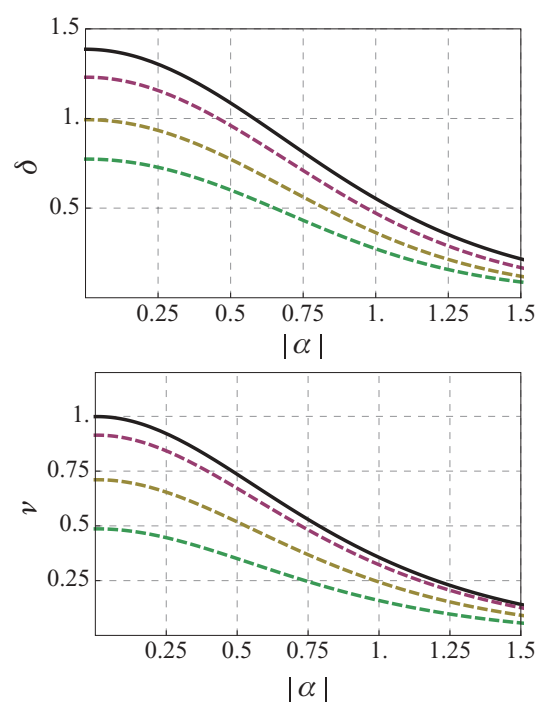

FIG. 2. (Color online) Non-Gaussianity $\delta[\varrho]$ (upper panel) and nonclassicality $\nu[\varrho]$ (lower panel) as a function of the amplitude $|\alpha|$ of the input coherent state for different values of the squeezing parameter r (dashed lines); from top to bottom $r = \{0.15, 0.30, 0.45\}$. The black solid line corresponds to the non-Gaussianity of the ideal photon-added coherent state; that is, to the limit $r \to 0$.

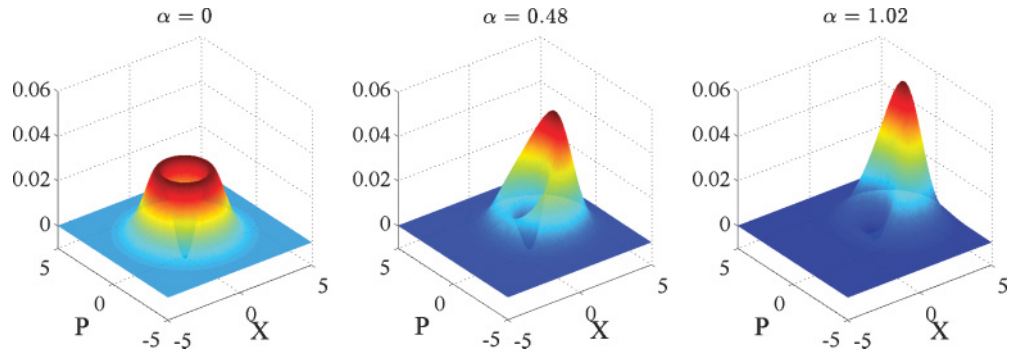

FIG. 3. (Color online) Experimental Wigner functions for increasing values of α. The output states are reconstructed by a maximal likelihood algorithm [50] which interpolates 800 000 data points sorted according to their phase into 12 histograms. The effectiveness of the sorting algorithm sets a lower bound $|\alpha| \sim 0.5$, so that the oscillations due to interference are much larger than low-frequency noise fluctuations. Notice that, for $\|\alpha\| = 0$, this noise can be compensated by using a moving-average technique.

nonclassical and thus useful for quantum information processing. It can be also observed how both non-Gaussianity and nonclassicality decrease by increasing the squeezing parameter; this can be explained by observing that, as shown in Eq. (4), for low values of r, the squeezing operator adds only one photon to each arm, while by increasing r we also have to consider the possible addition of many photons. Due to the lack of photon number resolution, the detection will be affected by the presence of higher-number emission from the squeezing process [Eq. (3)]. In this case, conditioned on a click from the idler beam, the signal will be in a highly mixed and thus less non-Gaussian and also nonclassical state. In the ideal limit of $r \to 0$, the non-Gaussianity of the state is exactly equal to that of the ideal photon-added coherent state in Eq. (5). However, this occurs at the expense of the success rate, and a compromise between non-Gaussianity and count rate has to be found.

Beside the role played by squeezing, we have to take into account the other imperfections that are present in our experimental setup. In the OPA there might occur a certain modal mismatch between the pump and the input: this results in a parasitic amplification that introduces excess noise on the signal and idler modes. The process is modelled as a nondegenerate OPA driven at a weaker strength γr, where $0 \leqslant \gamma \leqslant 1$ and $\gamma \sim 0.425$ in our experiment. The amplification couples the modes s and i with two other modes s' and i', initially in the vacuum state. The complete description takes the form

$$S_{s,i}(r)S_{s,i'}(\gamma r)S_{s',i}(\gamma r)|\alpha\rangle_s|0\rangle_i|0\rangle_{s'}|0\rangle_{i'}. \tag{6}$$

The parasite modes s' and i' are not observed in the experiment; therefore, we have to trace over them to obtain the output density matrix.

Accurate spatial and spectral filtering is performed so that the mode detected by the APD is matched with the input mode, which we detect by balanced homodyne; nevertheless, this task can be accomplished with only a limited efficiency ξ which, in our setup, takes the value $\xi \sim 0.96$. In formulas, we will have an output state $\varrho_{s,\surd}$ on the signal mode when the trigger count comes from the correct mode and a different state $\varrho_{s,\mathrm{x}}$ heralded by a faulty trigger event. The overall state is

$$\xi\varrho_{s,\surd} + (1-\xi)\varrho_{s,\mathrm{x}}. \tag{7}$$

Notice that dark count rates from the APD play a negligible role ($\sim$10 counts/s with an overall rate $\sim$1–4 $\times$ 10^3 counts/s), as we used a gated detection triggered by the cavity-dumping electronics of our laser. Homodyne detection has a limited efficiency as well, coming from optical loss, non-unit detector yield, and mode matching between the local oscillator and the signal. The overall efficiency is, in our case, of the order of $\eta \sim 0.71$; this is modelled as transmission through a beam splitter with transmissivity $t^2 = \eta$. Examples of the measured Wigner quasi-distributions are illustrated in Fig. 3.

In Fig. 4 we plot $\delta[\varrho]$ at fixed values of the coherent state amplitude $\alpha = 0.5$ and of the squeezing parameter $r = 0.15$ as a function, respectively, of the noise parameters γ, ξ, and η chosen in ranges relevant for our experimental setup. We observe as expected that $\delta[\varrho]$ decreases monotonically with γ, while it increases monotonically with ξ and η. For the values that characterize our experiment, the homodyne efficiency η is the source of imperfection that affects in the most detrimental way the non-Gaussianity of our states.

Finally, we evaluated $\delta[\varrho]$ from the experimentally reconstructed output states for different coherent state amplitudes

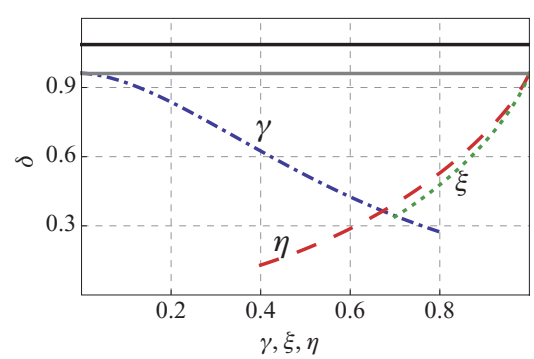

FIG. 4. (Color online) Non-Gaussianity $\delta[\varrho]$ as a function of the noise parameters of the experimental setup for fixed amplitude $|\alpha| = 0.5$ and squeezing parameter $r = 0.15$. In details: the blue dot-dashed line corresponds to $\delta[\varrho]$ as a function of γ, the green dotted line as a function of ξ, and the red dashed line as a function of η. The solid lines refer to the non-Gaussianity of the ideal photon-added coherent state with $|\alpha| = 0.5$ (upper black line) and to the non-Gaussianity of the state obtained by considering $|\alpha| = 0.5$, squeezing parameter $r = 0.15$, and no imperfections (lower grey line).

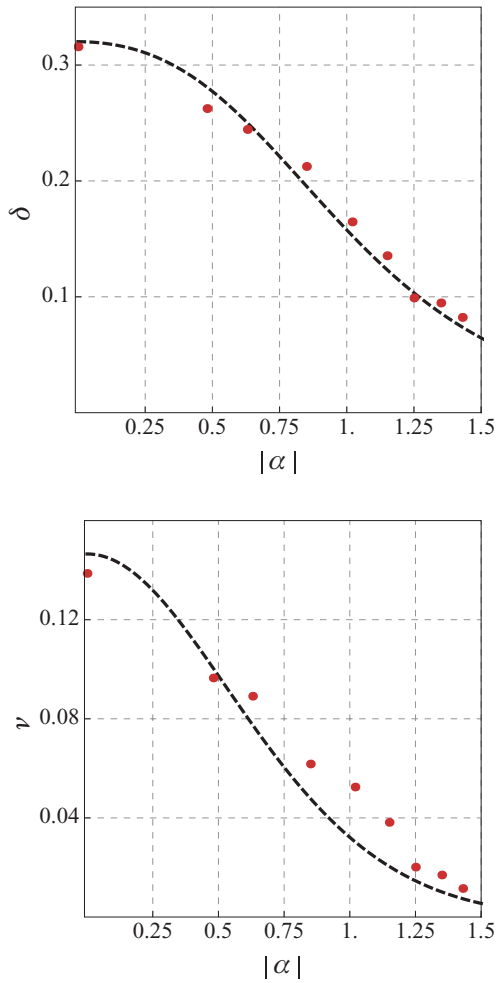

FIG. 5. (Color online) (Top) Non-Gaussianity $\delta[\varrho]$ as a function of the amplitude $|\alpha|$ of the input coherent state. (Bottom) Nonclassicality $\nu[\varrho]$—related to the minimum value of the Wigner function of ϱ—as a function of α. The red points are the experimental values from the reconstructed matrices. The black dashed line is obtained from our model including the main experimental imperfections of our implementation. The parameters are chosen in such a way as to fit the data of the non-Gaussianity: $r = 0.105$, $\gamma = 0.425$, $\xi = 0.96$, and $\eta = 0.71$.

$|\alpha|$; the results are shown in the upper panel of Fig. 5. The dashed line shows the description provided by our model when taking into account all the noise processes described above. The values of parameters used for the curve are obtained from a fit of the experimental data: $r = 0.105$, $\gamma = 0.425$, $\xi = 0.96$, and $\eta = 0.71$. The average fidelity between the reconstructed and modelled state is 0.989 ± 0.006 [51]. Concerning the non-Gaussianity, the agreement between the experimental data and the model is satisfactory, and we can observe, as expected, a decrease as the input intensity $|\alpha|$ increases. As shown, the effect of the single-photon addition is more relevant for quantum states with a small number of photons and becomes only a small perturbation for a higher average photon number.

In the lower panel of Fig. 5 we observe the behavior of $\nu[\varrho]$ as a function of the amplitude α. The experimental results confirm that the two quantities, non-Gaussianity and nonclassicality, have a similar behavior and that the non-Gaussianity induced by this photon-addition operation is essentially nonclassical. As a general remark, we notice that the logarithmic term in the expression (1) amplifies the effect of small discrepancies with the model we present. This qualifies our measure as a very sensitive one in those contexts where a good estimation of information resources is needed. In any case, our model is able to capture the essential features of the process, and provides us a tool to quantify how detrimental the imperfections are for the generation of these non-Gaussian resources.

IV. CONCLUSION

In summary, these experiments on single-photon-added coherent states demonstrate the relevance of this proposed measure of the non-Gaussianity. This measure appears as a reliable and sensitive way to quantify experimental imperfections of de-Gaussification experiments. It furthermore allows a link between non-Gaussianity and nonclassicality to be exhibited in such experiments. More generally, it would be useful to have a quantity available able to capture both features, non-Gaussianity together with nonclassicality, for any generic quantum states. Work along these lines is in progress and results will be developed elsewhere.

ACKNOWLEDGMENTS

We thank A. Ourjoumtsev, S. Olivares, F. Fuchs, F. Sciarrino, and F. De Martini for discussion. This work is supported by the EU project COMPAS, the ANR SEQURE, and partially by the CNISM-CNR agreement. M.B. is supported by the Marie Curie contract PIEF-GA-2009-236345-PROMETEO. F.F. is supported by CNano-Ile de France.

[1] S. L. Braunstein and P. van Loock, Rev. Mod. Phys. **77**, 513 (2005).
[2] S. L. Braunstein and H. J. Kimble, Phys. Rev. Lett. **80**, 869 (1998).
[3] A. Furusawa, J. L. Sørensen, S. L. Braunstein, C. A. Fuchs, H. J. Kimble, and E. S. Polzik, Science **282**, 706 (1998).
[4] S. L. Braunstein, N. J. Cerf, S. Iblisdir, P. van Loock, and S. Massar, Phys. Rev. Lett. **86**, 4938 (2001).
[5] P. T. Cochrane, T. C. Ralph, and A. Dolińska, Phys. Rev. A **69**, 042313 (2004).
[6] U. L. Andersen, V. Josse, and G. Leuchs, Phys. Rev. Lett. **94**, 240503 (2005).
[7] M. Ban, J. Opt. B: Quantum Semiclass. Opt. **1**, L9 (1999).
[8] S. L. Braunstein and H. J. Kimble, Phys. Rev. A **61**, 042302 (2000).
[9] X. Li, Q. Pan, J. Jing, J. Zhang, C. Xie, and K. Peng, Phys. Rev. Lett. **88**, 047904 (2002).
[10] T. C. Ralph, A. Gilchrist, G. J. Milburn, W. J. Munro, and S. Glancy, Phys. Rev. A **68**, 042319 (2003).
[11] A. Lund, T. C. Ralph, and H. L. Haselgrove, Phys. Rev. Lett. **100**, 030503 (2008).

[12] T. Opatrný, G. Kurizki, and D. G. Welsch, Phys. Rev. A **61**, 032302 (2000).
[13] P. T. Cochrane, T. C. Ralph, and G. J. Milburn, Phys. Rev. A **65**, 062306 (2002).
[14] S. Olivares, M. G. A. Paris, and R. Bonifacio, Phys. Rev. A **67**, 032314 (2003).
[15] N. J. Cerf, O. Krüger, P. Navez, R. F. Werner, and M. M. Wolf, Phys. Rev. Lett. **95**, 070501 (2005).
[16] F. Casagrande, A. Lulli, and M. G. A. Paris, Phys. Rev. A **75**, 032336 (2007).
[17] A. I. Lvovsky, H. Hansen, T. Aichele, O. Benson, J. Mlynek, and S. Schiller, Phys. Rev. Lett. **87**, 050402 (2001).
[18] J. Wenger, R. Tualle-Brouri, and P. Grangier, Phys. Rev. Lett. **92**, 153601 (2004).
[19] A. Zavatta, S. Viciani, and M. Bellini, Phys. Rev. A **70**, 053821 (2004).
[20] A. Ourjoumtsev, R. Tualle-Brouri, and P. Grangier, Phys. Rev. Lett. **96**, 213601 (2006).
[21] A. Ourjoumtsev, R. Tualle-Brouri, J. Laurat, and P. Grangier, Science **312**, 83 (2006).
[22] J. S. Neergard-Nielsen, B. M. Nielsen, C. Hettich, K. Molmer, and E. S. Polzik, Phys. Rev. Lett. **97**, 083604 (2006).
[23] A. Ourjoumtsev, H. Jeong, R. Tualle-Brouri, and P. Grangier, Nature (London) **448**, 784 (2007).
[24] M. S. Kim, J. Phys. B **41**, 133001 (2008).
[25] A. Ourjoumtsev, F. Ferreyrol, R. Tualle-Brouri, and P. Grangier, Nature Phys. **5**, 189 (2009).
[26] V. D'Auria, A. Chiummo, M. De Laurentis, A. Porzio, S. Solimeno, and M. G. A. Paris, Opt. Express **13**, 948 (2005).
[27] V. D'Auria, C. de Lisio, A. Porzio, S. Solimeno, J. Anwar, and M. G. A. Paris, Phys. Rev. A **81**, 033846 (2010).
[28] S. Deléglise *et al.*, Nature (London) **455**, 510 (2008).
[29] M. Hofheinz *et al.*, Nature (London) **454**, 310 (2008).
[30] A. Ourjoumtsev, A. Dantan, R. Tualle-Brouri, and P. Grangier, Phys. Rev. Lett. **98**, 030502 (2007).
[31] H. Takahashi *et al.*, Nature Phot. **4**, 178 (2010).
[32] F. Ferreyrol, M. Barbieri, R. Blandino, S. Fossier, R. Tualle-Brouri, and P. Grangier, Phys. Rev. Lett. **104**, 123603 (2010).
[33] G. Y. Xiang, T. C. Ralph, A. P. Lund, N. Walk, and G. J. Pryde, Nature Photon. **4**, 316 (2010).
[34] A. Allevi, A. Andreoni, M. Bondani, M. G. Genoni, and S. Olivares, Phys. Rev. A **82**, 013816 (2010).
[35] A. Zavatta, V. Parigi, and M. Bellini, Phys. Rev. A **75**, 052106 (2007).
[36] V. Parigi, A. Zavatta, M. S. Kim, and M. Bellini, Science **317**, 1890 (2007).
[37] A. Zavatta, V. Parigi, M. S. Kim, H. Jeong, and M. Bellini, Phys. Rev. Lett. **103**, 140406 (2009).
[38] E. Shchukin, Th. Richter, and W. Vogel, Phys. Rev. A **71**, 011802 (2005).
[39] T. Kiesel, W. Vogel, V. Parigi, A. Zavatta, and M. Bellini, Phys. Rev. A **78**, 021804 (2008).
[40] T. Kiesel, W. Vogel, B. Hage, J. DiGuglielmo, A. Samblowski, and R. Schnabel, Phys. Rev. A **79**, 022122 (2009).
[41] N. Spagnolo, C. Vitelli, T. De Angelis, F. Sciarrino, and F. De Martini, Phys. Rev. A **80**, 032318 (2009).
[42] M. G. Genoni, M. G. A. Paris, and K. Banaszek, Phys. Rev. A **78**, 060303 (2008).
[43] M. G. Genoni and M. G. A. Paris, Phys. Rev. A **82**, 052341 (2010).
[44] A. S. Holevo, M. Sohma, and O. Hirota, Phys. Rev. A **59**, 1820 (1999).
[45] M. G. Genoni, M. G. A. Paris, and K. Banaszek, Phys. Rev. A **76**, 042327 (2007).
[46] V. V. Dodonov, O. Manko, V. Manko, and A. Wunsche, J. Mod. Opt. **47**, 633 (2000).
[47] V. V. Dodonov and M. B. Renò, Phys. Lett. A **308**, 249 (2003).
[48] P. Marian, T. A. Marian, and H. Scutaru, Phys. Rev. A **69**, 022104 (2004).
[49] A. Mari, K. Kieling, B. Melholt Nielsen, E. S. Polzik, J. Eisert, e-print arXiv:1005.1665v2 [quant-ph].
[50] A. I. Lvovsky, J. Opt. B: Quantum Semiclass. Opt. **6**, S556 (2004).
[51] Here, we use the definition of the fidelity F between two states ϱ_1 and ϱ_2: $F=\mathrm{Tr}^2(\sqrt{\varrho_1}\varrho_2\sqrt{\varrho_1})^{1/2}$.